An Investigation into Radio Interferometry

Elisha Jhoti
March 26, 2017

ABSTRACT

The aims of this investigation were to find values for the components of the Campbell Hall interferometer baseline using least squares fitting of point source, (the Orion Nebula), and extended source, (the Sun and Moon) data, as well as values for the diameters of the Sun and Moon. The least squares fit on the Sun data gave a value for the East-West component of the baseline of 16.2m. The least squares fit of the point source data gave a value for the East-West component of the baseline of 15.4m. The 2D fit of the point source data did not give accurate results, the same as with the diameters of the Sun and Moon.

Contents

1. Introduction and Background

Radio interferometry is the basis for most radio astronomy today. For this investigation we used an interferometer operating at about 12GHz. It consists of two telescope dishes that each receive a signal, these are then multiplied together using a mixer. The baseline, B, is the distance between these two dishes, this is made up of two components, $B_{ew} \approx 20m$, (the East-west component), and $B_{ns} \approx 1m$, (the North-South component). The output of the interferometer is a sine-like signal known as the fringe, this contains information about the source in its frequency, amplitude and phase. With our baseline, we get a fringe spacing of approximately 5', since fringe spacing $= \frac{\lambda}{B}$, where λ is the wavelength of the signal.
For this investigation we looked at a point source, the Orion Nebula, with $ra = 05^h35^m17.3s, dec = -0.5°23'28''$, as well as two extended sources: the Sun and Moon. The Orion nebula is a region where hot stars have produced ionised gas, this emits radiation known as free-free radiation, caused by electrons deflecting off protons. On the other hand, the Moon, unlike popular belief, does not shine due to reflected light from the Sun, rather it emits blackbody radiation from its surface, which is heated by the Sun. Using the fringe of a horizon-to-horizon measurement of the Sun or Moon, we can infer their diameters and baselines, B_{ew} and B_{ns}.

2. Experiments and Observations

2.1. Point Source Observation

First we did a measurement of the Sun for one hour to ensure the system was working properly. Then we did a horizon-to-horizon measurement of the point source. We had to precess the coordinates to the current equinox using the IDL procedure `precess` to get the correct ra's.

2.2. Sun and Moon Observation

Next we took a horizon-to-horizon measurement of the Sun. Unfortunately, we calculated the duration of the measurement incorrectly, and so approximately one hour is missing from the middle of the data, this may affect the analysis. We also did a horizon-to-horizon measurement of the Moon. We used the IDL function `follow` and set the keywords `moon` and `sun` respectively, this points the interferometer to follow the paths of the Moon and Sun.

3. Data Analysis

3.1. Point Source Analysis

The main goal for this investigation in the study of the point source is to find values for the baseline components, B_{ew} and B_{ns}, using a least squares fit on the fringe. The two telescopes have different distances to the source as it moves through the sky, this results in a time dependant path delay, τ_g . There are also delays introduced by the cable system in the electronics, τ_c, which is independant of time. The total delay is just the sum of the two. τ_g can be split into the same components as the baseline; East-West and North-South. Through geometry we can relate these to the baseline components, hour angle and declination.

$$\tau_{g,ew}(h_s) = [\frac{B_{ew}}{c} cos\delta] sinh_s \tag{1}$$

$$\tau_{g,ns}(h_s) = [\frac{B_{ns}}{c} sinLcos\delta] cosh_s - [\frac{B_{ns}}{c} cosLsin\delta] \tag{2}$$

Where L is the latitutde of the telescopes. The first term in Equation 2 is the delay perpendicular to the Earth's axis, the second is the delay parallel to the Earth's axis, since this has no hour angle dependance we can combine it with the cable delay, τ_c.

$$\tau_g'(h_s) = [\frac{B_{ew}}{c} cos\delta] sinh_s + [\frac{B_{ns}}{c} sinLcos\delta] cosh_s \tag{3}$$

The output of the interferometer is the product of the two signals from the telescopes, using trignometric identities we can express this as:

$$F(h_s) = cos(2\pi\nu\tau_c) cos(2\pi\nu\tau_g') - sin(2\pi\nu\tau_c) sin(2\pi\nu\tau_g') \tag{4}$$

We can express the delay in units of wavelength, λ, and then subsitute it into Equation 4 to get an equation for fringe amplitude, $F(h_s)$.

$$\nu\tau_g'(B_{ew}, B_{ns}, \delta, h_s) = [\frac{B_{ew}}{\lambda} cos\delta] sinh_s + [\frac{B_{ns}}{\lambda} sinLcos\delta] cosh_s \tag{5}$$

$$F(h_s) = Acos(2\pi\nu\tau_g') + Bsin(2\pi\nu\tau_g') \tag{6}$$

Where A and B replace $cos(2\pi\nu\tau_c)$ and $-sin(2\pi\nu\tau_c)$ as the 'unknown' constants for the least squares fit.

In this case we use the 'Brute-Force Technique' for least squares fitting. First, we wrote software to apply a least squares fit on a 'flat' part of the horizon-to-horizon Sun data. We initially did a 1D fit where we only consider the B_{ew} component and approximate $B_{ns} = 0$. This involved iterating through guess values for B_{ew} and substituting them into Equation 5 until we find the minimum point of the sum-of-squares, this point gives the best value of B_{ew}, (see plots below), as the sum-of-squares gives the uncertainty in the fit.

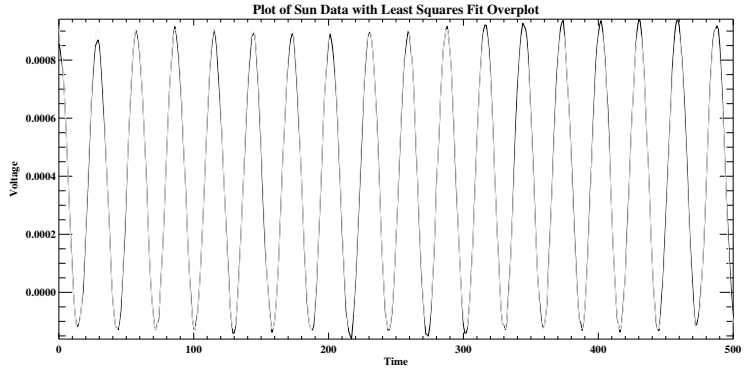

Fig. 1.— Plot showing a slice of flat Sun data with the fitted values overplotted with a dashed line.

As you can see in Figure 1, the fit is very exact over the data. This is because we chose a very smooth slice of the Sun data to apply the least squares fit on. By plotting the sum-of-squares against Q_{ew}, where $Q_{ew} = \frac{B_{ew}}{\lambda} cos\delta$, we found the minimum point and rearranged the equation for Q_{ew} to get the best value for B_{ew}, (see plot below).

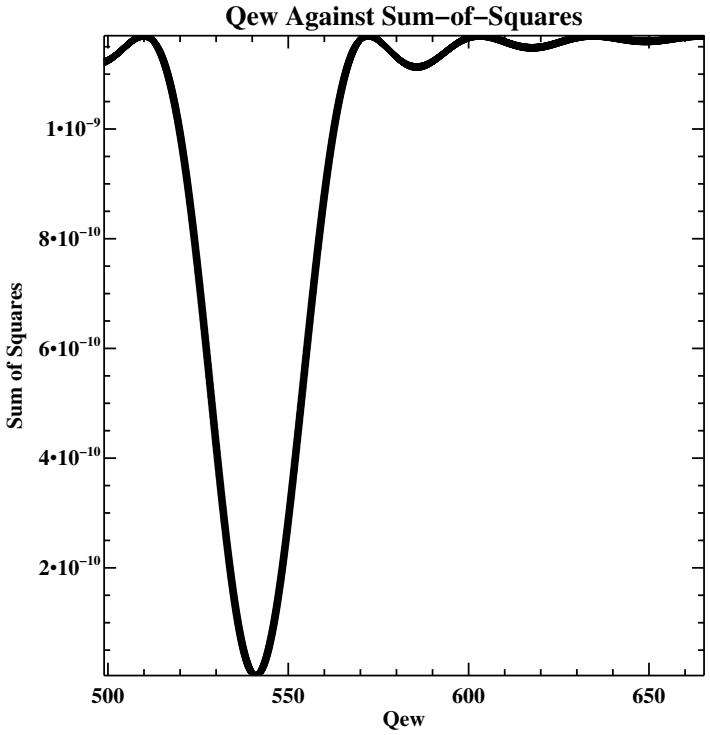

Fig. 2.— Plot showing the sum-of-squares against Q_{ew} where the minimum point gives the East-West component of the baseline.

This gives us a value for Q_{ew} of approximately 540, resulting in $B_{ew} = 16.2m(1d.p)$ Next we applied the same software on the point source data. Unfortunately the fit was not as exact as the Sun data fit, this may be because there were alot of possible sources of error and noise that would have affected the data, for example, the Campanile getting in the way of the signal. The plot of Q_{ew} against the sum-of-squares seems to have a false minimum which gives a B_{ew} value of 60m, this may also be due to the sources of error mentioned above. Ignoring, this minimum point, the next minimum would give $B_{ew} = 15.4m$ which is a bit more realistic, see the plots below.

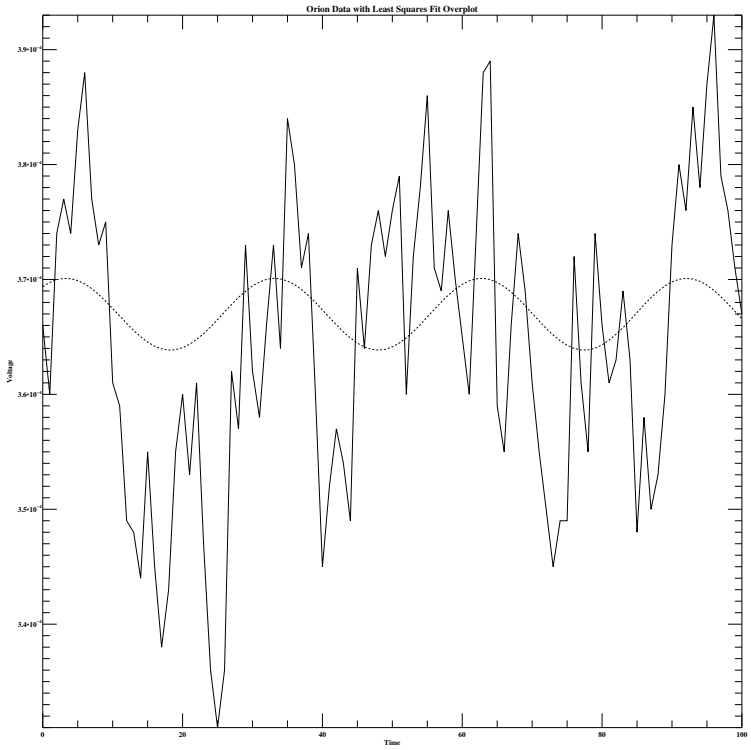

Fig. 3.— Plot showing the point source data with the least squares fit overplotted with a dashed line.

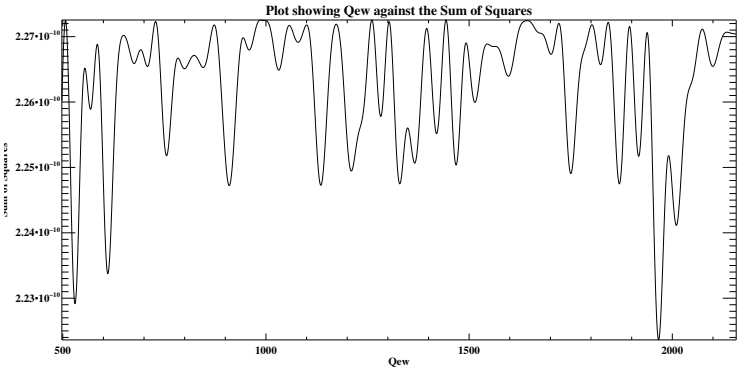

Fig. 4.— Plot showing Qew against the sum of squares, where the minimum should give the best Bew value, in this case it is most likely the second lowest peak

We also applied a 2D fit on the point source data by creating a 2D array and plotting a contour plot of the sum-of-squares array. If our data was accurate, this should have given the minimum of the 2D sum-of-squares matrix plotted as a darker, ellipse-shaped region. Unfornately, our fit is not that accurate so we only managed to obtain a straight rectangle-shaped minimum region, see the plot below.

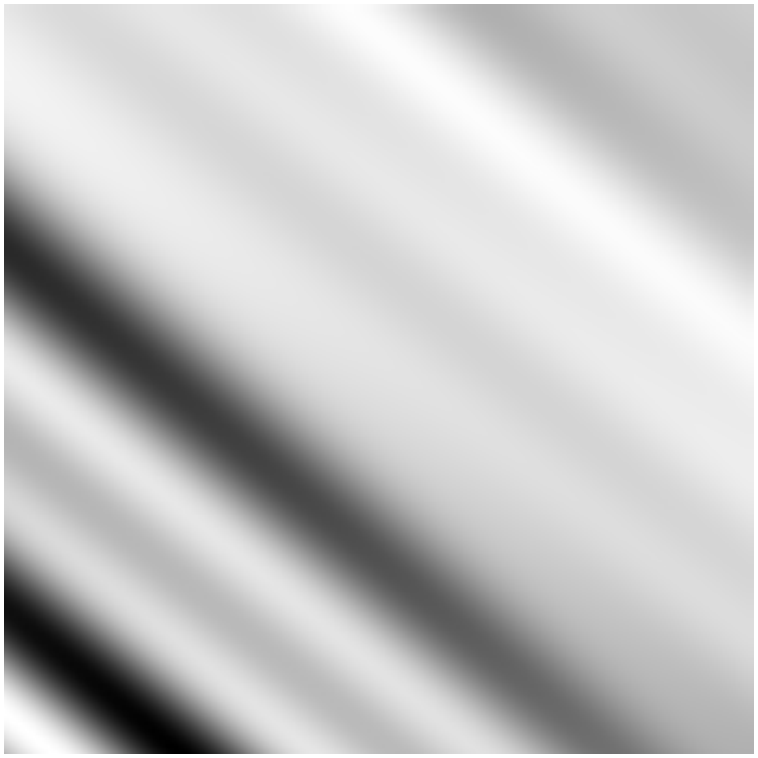

Fig. 5.— Contour plot of the 2D sum-of-squares array for the point source data. The minimum region should give the best value for the baseline.

We also found the fringe frequencies by plotting the power spectrum of the data. We did this for the 'test' Sun data (i.e. the measurement of the Sun in Section 2.1 that lasted for an hour), and used the equation below to find the fringe frequency for the point source data.

The local fringe frequency is given by the equation:

$$f_f = [\frac{B_{ew}}{\lambda} cos\delta] cosh_{s,0} - [\frac{B_{ns}}{\lambda} sinLcos\delta] sinh_{s,0} \tag{7}$$

Where $h_{s,0}$ is the initial hour angle of the source. Equation 7 gives fringe frequency in cycles per radian on the sky. It is the frequency at which the products in Equation 5 oscillate as the hour angle changes over time. This gives us a value of fringe frequency for the point source data of 0.048Hz.

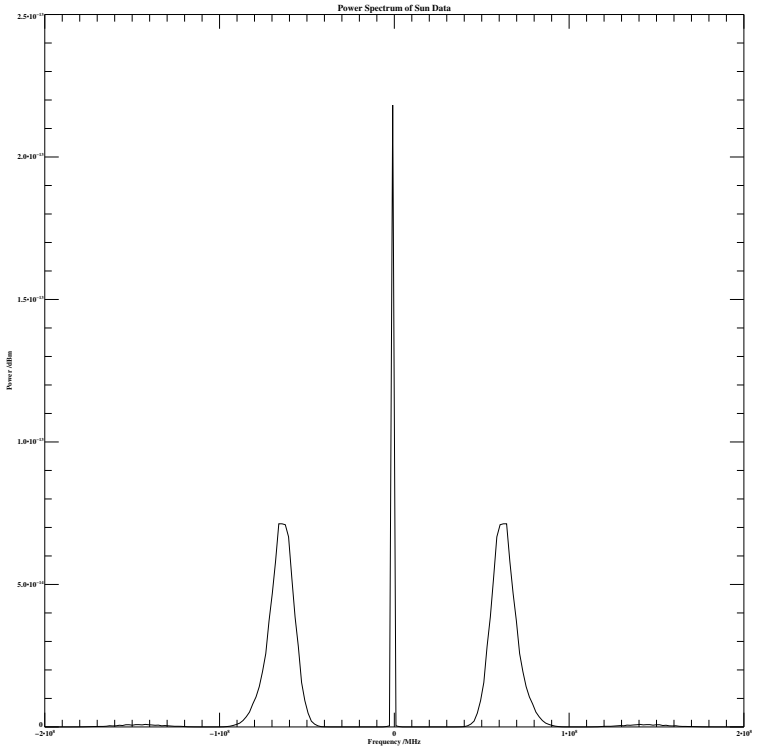

Fig. 6.— Power Spectrum of hour long Sun data showing fringe frequencies.

3.2. Sun and Moon Analysis

The main goal for measuring the Sun and Moon is to find values for their diameters. We have to assume they are both uniformly bright disks of radius R, which is not exactly true in reality. The interferometer response, $R(h_s)$, to an extended source, like the Sun or Moon, can be expressed as a product between the 'point source fringe'; Equation 6, and the fringe modulator, which multiplies this function and depends on the intensity and fringe frequencies.

$$R(h_s) = F(h_s) \times \int I(\Delta h) cos(2\pi f_f \Delta h) d\Delta h \tag{8}$$

Where $\Delta h = h = h_s$ is the hour angle, and h is the hour angle relative to the hour angle of the source centre, h_s. The fringe modulator is the Fourier transform of the source intensity distribution on the sky. For our purposes, we expressed the integral as a sum which runs from -N to +N where N is the number of datapoints.

$$MF_{theory} \approx \delta h \sum_{n=-N}^{n=+N} [1 - (\frac{n}{N}/N)^2]^{1/2} cos(\frac{2\pi f_f R n}{N}) \tag{9}$$

The modulating function goes through various zero points, which occur for $f_f = \frac{n}{2R}$, where R is the radius of the source. We can express this in terms of fringe period $\frac{1}{f_f} = \frac{2R}{n}$. In the end, we can get the radius of the source, R, by comparing MF_{theory} with $MF_{observed}$. This means, if we plot the power spectra of the Sun and the Moon, the zero points should give their diameters, (see plots below).

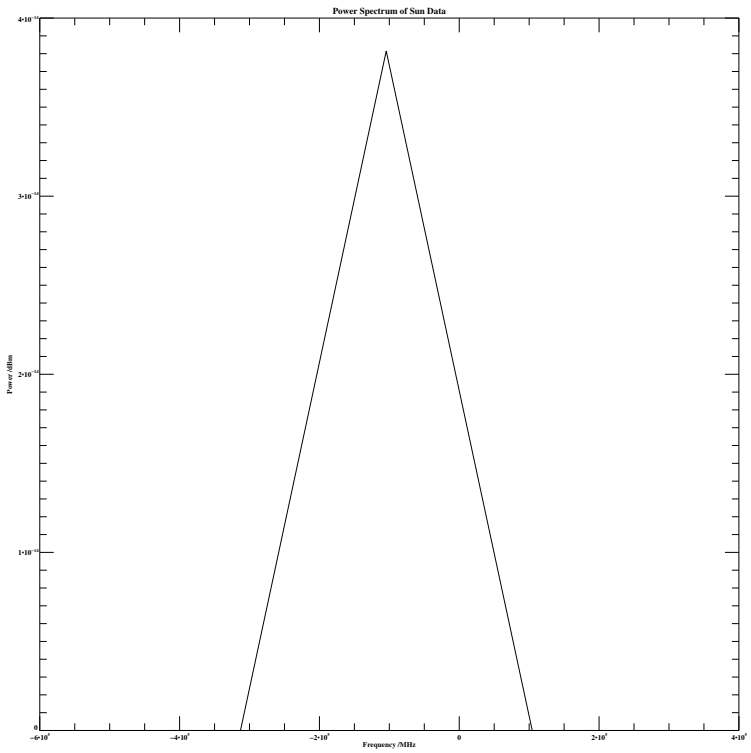

Fig. 7.— Power Spectrum of horizon-to-horizon Sun data. The zero points give the diameter.

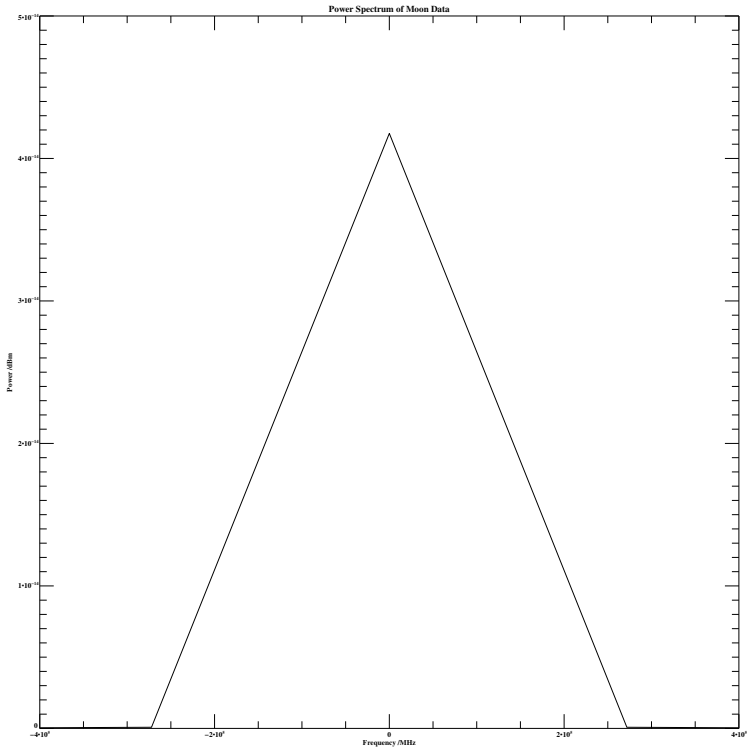

Fig. 8.— Power Spectrum of horizon-to-horizon Moon data. The zero points give the diameter.

These power spectra do not give values of the diameters that are accurate, suggesting something must be wrong with our data or the calculations are incorrect.

4. Interpretations and Conclusions

Our least squares fit on the Sun data seemed to give the most accurate value of the baseline: $B_{ew} = 16.2m$, since the true value is around 20m. This is probably because we only used a small slice of the data, therefore there was less room for error and contributions from outside sources such as hills and buildings that would have blocked the signal. The fact that Figure 2 gave such a clear minimum suggests the fit was very accurate. Unfortunately, the same cannot be said for the fit on the point source data. As you can see from Figure 3, the fitted values do not match the data very well at all. This is most likely because of inaccuracies in the data or in the calculations, for example; using too small a range of baseline guess values. Figure 4 confirms this interpretation as it seems to show a false minimum in the data that would give a value of the baseline that is much too large. The next lowest peak would give the correct baseline, $B_{ew} = 15.4m$ suggesting this is an anomalous datapoint. The contour plot reaffirms this as we can clearly see two minimum regions. However, neither are the correct shape that we expected, so would most likely not give us accurate values for both baseline componenets. Figure 6 gives a smooth power spectrum of the hour long Sun data, again telling us that a smaller slice of data gives more accurate results due to minimisation of anomalies. Usually this would not make sense, because in a smaller dataset anomalies would have a greater effect. However, since these measurements invlove tracking an object through the sky for prolonged periods of time, with no way to know if the source is blocked at any time during this measurement, the conclusion that a smaller slice of data would give more accurate results makes sense.
The Sun and Moon analysis is another example of this, since neither gave accurate values for their diameter and the whole dataset for each was used.

5. Challenges and Improvements

The main challenge for this investigation was writing the software for the least squares fit. With more time, this could have been improved, and perhaps a retake of the data would have yielded better results, especially in the case of the point source. Another improvement would be to retake the Sun and Moon horizon-to-horizon measurements in order to get better values for the diameters.

6. Programs

Below is a list of procedures and batch files used to analysise the data in this report. They can be found under the directory path /home/ejhoti/Astro121/lab3/week1 and /week2.

1. `fringefreq.pro`: Procedure that calculates the fringe frequency of the point source data and plots the power spectrum of the hour long Sun data.

2. `leastsquares.pro`: Procedure that applies 1D and 2D least squares fit using brute force technique on point source data.

3. `orionanalysis.batch.pro`: Batch file that plots the power spectrum of the point source data.

4. `diameter.pro`: Procedure that plots the power spectra of the Sun and Moon using the horizon-to-horizon data in order to find their diameters.

5. `sunanalysis.pro`: Procedure that applies 1D least squares fit using brute force technique on slice of Sun data.